

Differences in F9 and 5.51 cell elasticity determined by cell poking and atomic force microscopy

Wolfgang H. Goldmann^{a,*}, Reinhard Galneder^a, Markus Ludwig^b, Alexander Kromm^a, Robert M. Ezzell^a

^a*Surgery Research Unit, Department of Surgery, Massachusetts General Hospital, Harvard Medical School, Building 149, 13th Street, Charlestown, MA 02129, USA*

^b*Lehrstuhl für Angewandte Physik, Ludwig Maximilians University, D-80799 Munich, Germany*

Received 26 December 1997; revised version received 6 February 1998

Abstract We studied the elasticity of both a wild type (F9) mouse embryonic carcinoma and a vinculin-deficient (5.51) cell line, which was produced by chemical mutagenesis. Using cell poking, we measured the effects of loss of vinculin on the elastic properties of these cells. F9 cells were about 20% more resistant to indentation by the cell poker (a glass stylus) than were 5.51 cells. Using the atomic force microscope to map the elasticity of wild type and vinculin-deficient cells by 128×128 force scans, we observed a correlation of elasticity with cell poking elastometric measurements. These findings, as well as previous atomic force, rheologic, and magnetometric measurements [Goldmann and Ezzell, *Exp. Cell Res.* 226 (1996) 234–237; Ezzell et al., *Exp. Cell Res.* 231 (1997) 14–26], indicate that vinculin is an integral part of the cytoskeletal network.

© 1998 Federation of European Biochemical Societies.

Key words: Vinculin-regulated cellular elasticity

1. Introduction

Actin membrane attachment is one of the principal mechanisms by which cells determine their shape, attach to surfaces, and direct their motility. A protein known to be involved in this linkage in epithelial cells is vinculin [1]. We have been studying a mouse embryonic carcinoma F9 cell line, which was produced by chemical mutagenesis to contain no detectable vinculin protein (called 5.51), that adheres poorly to substrates and does not differentiate into a polarized epithelium [2]. In extensive studies, we have characterized the motile behavior, mechanical properties, and the expression and localization of focal adhesion complex proteins in 5.51 cells, comparing these with the properties of wild type (F9) cells [3–5]. We found that the loss of vinculin brings about a marked reduction in cell adhesion, shape change, spreading and stiffness, as well as an increase in surface motility and locomotion. We have also examined another vinculin-deficient F9 cell line, F9Vin(–/–), which was created by targeting both vinculin genes using homologous recombination [6,7]. The adhesion of these cells is only slightly less inhibited than that of the 5.51 cells. In recent atomic force microscopic (AFM) measurements, we showed that the elasticity in F9Vin(–/–) cells is reduced approximately 20% from that of the wild type, and

we demonstrated the elastic distribution by three-dimensional image analysis [8].

In this study, we used cell poking elastometry as well as atomic force microscopy to elucidate the influence of vinculin on the elastic properties of 5.51 cells. We present evidence using 3D image analysis that vinculin-deficient cells are notably softer, i.e. less resistant, to force by the cell poker and the AFM cantilever than are wild type cells. We propose that lack of vinculin has a similar influence on the elasticity of both 5.51 and F9Vin(–/–) cells and hypothesize that this protein is a key element in connecting the cytoskeleton to the lipid membrane to bring about physical changes.

2. Materials and methods

2.1. Cell line and culture

The 5.51 cell line, produced by ethylmethanesulfonate (EMS) mutagenesis, is deficient in vinculin and expresses only 30–50% uvomorulin [2]. The wild type (F9) cells were maintained on 0.1% gelatin-coated charged plastic culture dishes in high-glucose (4.5 g/l) Dulbecco's modified Eagle's medium supplemented with 10% calf serum, 20 mM HEPES, 2 mM L-glutamine, and 100 U/ml penicillin-streptomycin (P/S). 5.51 cells were grown in suspension in the same medium.

2.2. Reflection interference contrast (RICM), laser confocal, and video microscopy

RICM was carried out as described by Schindl et al. [9]. In brief, the system consists of a Zeiss Axiomat inverted microscope containing a $63\times$ antilex Neofluar objective, a mercury arc lamp, and custom optics for observing RICM and bright-field images alternatively or in parallel. Filters are used to reduce exposure of ultraviolet and infrared light and to select the 546 nm green mercury line. The interference images are captured using a CCD camera.

For three-dimensional reconstruction of the confocal images, 10 optical sections at 1–2 μm intervals of the entire thickness of the cell were collected using a Zeiss IM35 inverted microscope, a $100\times$ Planeo fluor objective, a Bio-Rad MRC 600 confocal microscope, and COMOS software. The stack of confocal images was then compiled and rendered using Image-1 software running on a 486 50 MHz PC.

The analog video signal was digitized by a PixelTools video digitizing card (Perceptics, Knoxville, TN) and processed by an Apple Macintosh Quadra 950 equipped with an accelerated video display card (Futura LX, Radius, Sunnyvale, CA). Image analysis was carried out using Image VDM Software (Perceptics) based on the Public Domain Image processing software 'NIH Image' (written by Wayne Rasban, NIH, Bethesda, MD).

2.3. Cell poking elastometry

The cell poking elastometer is a purpose-built apparatus which was developed by Ziegler [10], based on the work of Duszyk et al. [11] and applied by Schultheiss [12]. A schematic view of the cell poking device, illustrating the basic principle, is given in Fig. 1A. In short, this instrument is mounted on an inverted microscope that allows accurate three-dimensional lateral positioning (within 1 nm precision) of the glass stylus. The cells are plated on glass coverslips which were coated with 5 $\mu\text{g}/\text{cm}^2$ human fibronectin and 1 $\mu\text{g}/\text{cm}^2$ poly-D-lysine. The

*Corresponding author. Fax: (1) (617) 726 5669.
E-mail: goldman@helix.mgh.harvard.edu

Abbreviations: F9, a wild type mouse embryonic carcinoma cell line; 5.51, a F9 cell line deficient in vinculin generated by chemical mutagenesis; F9Vin(–/–), a F9 cell line deficient in vinculin, in which both vinculin genes are inactivated by homologous recombination

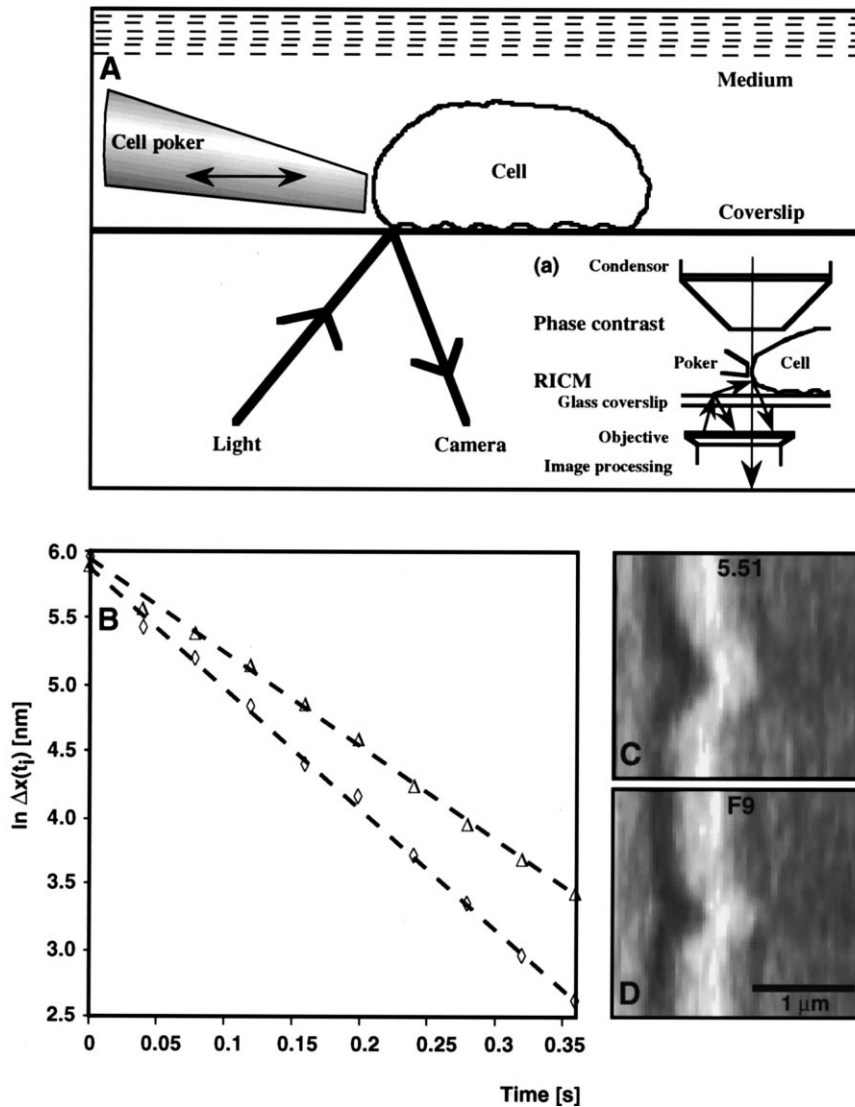


Fig. 1. A basic schematic representation of the cell poking device (A). The relaxation decay of the cell membrane laterally indented by a glass stylus which is instantaneously withdrawn is monitored. Under epi-illumination using monochromatic light, the interference fringes (bright-field mode) from the difference in the optical path between the object and the glass interface are video-recorded and analyzed (a, inset). The rate of relaxation was determined from the analysis of 10 video frames using the relation $\ln \Delta(t_i) = -k \times t_i$ with $k = 9.0 \text{ s}^{-1}$ for the F9 (diamonds) and $k = 7.1 \text{ s}^{-1}$ for the 5.51 (triangles) cell (B). Bright-field images taken after poking a F9 and a 5.51 cell membrane and immediately retracting the glass stylus at $t_i = 0 \text{ s}$ (C and D). Ten separate measurements per cell line were carried out which showed a standard deviation of less than 5%. Bar = 1 μm .

combination of both fibronectin and poly-D-lysine was necessary to attach the non-adherent 5.51 cells to coverslips. The deformation of the cell membrane by the glass stylus is measured by RICM and bright-field optics after instantaneous computer-controlled retraction of the glass poker up to 5 μm (Fig. 1A,a). The following relaxation process is captured in 10 individual video frames. To describe the elastic response of F9 cells attached to fibronectin and poly-D-lysine coated coverslips, the following equation is used: $\ln \Delta(t_i) = -k \times t_i$, where $\Delta x(t_i)$ = time-dependent 'lateral deformation' relaxation (nm), and k = rate of relaxation (s). Plotting $\Delta x(t_i)$ against time t_i yields the decay of the indentation, with k being a measure of the cell's elasticity (Fig. 1B) [12].

2.4. Atomic force microscopy

The wild type (F9) and vinculin-deficient (5.51) cell lines were cultured for 8 h on 2 $\mu\text{g/ml}$ poly-D-lysine coated 35 \times 15 mm Nunc dishes. Prior to experimentation, the dishes were rinsed with PBS to remove non-adherent cells. The atomic force microscope is a home-built instrument [13]. In brief, this instrument is combined with an epi-light microscope that allows the exact positioning of the cantilever

tip. The deflection of the cantilever is measured by a position-sensitive two-segment photo diode, and the extent to which the applied force indents the cells depends on their elastic properties. The Hertz model is used to describe the elastic response of F9 and 5.51 cells indented by the AFM cantilever, which predicts a relation between indentation and loading force. The image area is determined by 128 \times 128 pixels. At each pixel point, the deflection signal of the cantilever is analyzed for the topography and elasticity of the cell. The variation in 0–255 'elastic' scales and the images are generated by transferring the data into gray scales, where 0 corresponds to soft and 255 to hard. Three-dimensional profiles are generated by a customized processing software, 'Image 1.41b20 (non FFT)' and Adobe Photoshop 3.0.

3. Results

3.1. Cell poking

Prior to cell poking, we used light microscopy to examine the attachment and spreading of the (F9) wild type and (5.51)

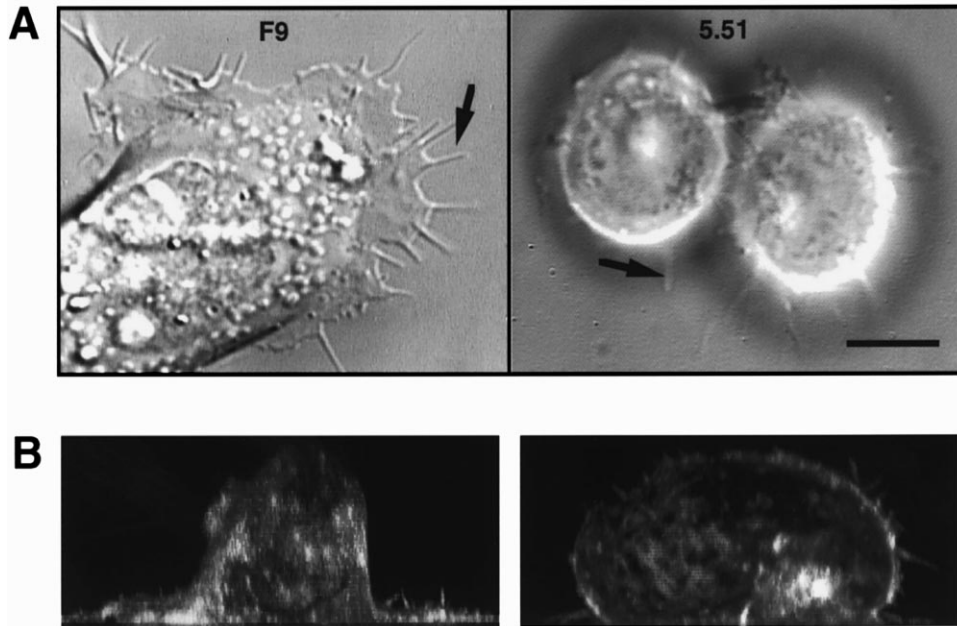


Fig. 2. Spreading of wild type (F9) and vinculin-deficient (5.51) cells, cultured on fibronectin and poly-D-lysine coated coverslips and examined with video-enhanced Nomarski DIC optics. The F9 cell has lamellipodia and extending filopodia. The 5.51 cells are less spread than the wild type cell, have no lamellipodia but have a few filopodia (arrows in A) that extend further out than those in the wild type cell. Three-dimensional reconstruction of confocal images of a F9 and 5.51 cell are shown in B. The images were created by compiling digitized sections at a 90° view of the cells. Bar = 5 µm.

vinculin-deficient cells to fibronectin and poly-D-lysine coated coverslips (Fig. 2A). The wild type cells exhibited veil-like lamellipodia and many filopodia; in contrast, 5.51 cells had few filopodia but no lamellipodia [3,4,14]. This is confirmed by a lateral view at a 90° angle showing the elongated shape and widely spread ventral surface of the wild type cell, and the

spherical shape and lack of lamellipodia in the 5.51 cell (Fig. 2B). In a typical cell poking experiment, a fine glass stylus is used to indent the cell by 0.35 µm (Fig. 1A). After immediate retraction of the glass stylus, the relaxation decay of the indentation is recorded in bright-field mode by video (Fig. 1A,a). Fig. 1C,D depicts the membrane deformation of a

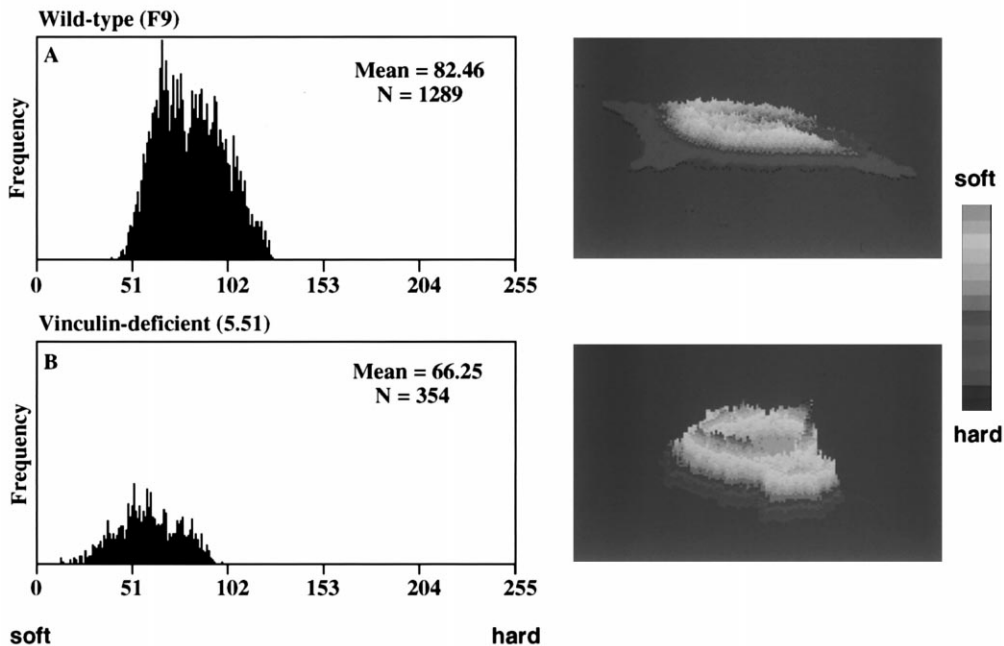


Fig. 3. Results from AFM measurements in histogram and 3D image form for the F9 (A) and 5.51 cell (B). The profiles were generated by 128×128 force scans of the cantilever which are transformed in 256 scales (histogram) and 3D images. As indicated by the gray scale (on the right), the wild type cell is less deformable by the cantilever than is the 5.51 cell. The lack of vinculin in the 5.51 cell is reflected by a shift toward the softer region (histogram). This result is consistent with magnetometry data [14]. An average of (n=3) separate measurements per cell line were performed which showed a standard deviation of < 3%.

5.51 and wild type cell after poking at $t_i = 0$ s. Compared to the membrane of the wild type, the membrane of the vinculin-deficient cell is clearly indented over a wider area, indicating less resistance to mechanical force. Analyzing the deformation process from an average of 10 frames taken at a frequency of 25 Hz, we calculated a relaxation rate of 9 s^{-1} and 7.1 s^{-1} for (F9) wild type (diamonds, Fig. 1B) and for (5.51) vinculin-deficient cells (triangles, Fig. 1B), respectively. Interestingly, Schultheiss [12] has also reported a rate of relaxation of 6.7 s^{-1} for human erythrocytes under identical experimental conditions.

3.2. Atomic force microscopy

In our AFM experiments, the cantilever tip raster-scans across the cell surface and creates an image of the cells which is made up of 128×128 (= 16384) data points. These points are then converted into 256 scales to produce a topographic image and to quantify the elasticity of the cell. Fig. 3 shows the elastic distribution of a wild type and a vinculin-deficient cell in histogram form where 0 represents soft and 255 represents hard and the corresponding three-dimensional profiles in gray scales. As indicated by the histogram and gray scale, the wild type cell is less deformed by the cantilever and thus harder in comparison with the vinculin-deficient cell. The total area of the 5.51 cell shows only about 28% of the F9 cell level, as well as reduced filopodia and no lamellipodia, which compares well with the light microscope images in Fig. 2A,B.

4. Discussion

In this work we have examined the influence of vinculin on the elastic properties of 5.51 cells using cell poking elastometry and atomic force microscopy. It has been postulated that transmembrane force transfer across integrins correlates with the recruitment of focal adhesion complex proteins [15], which include vinculin, and thus, correlates also with physical linkage to the actin cytoskeleton. Our data from cell poking and atomic force measurements are in agreement insofar as the vinculin-deficient 5.51 cells reflect changes in phenotype. Shape changes are generally mediated through cytoskeletal reorganization i.e. binding of actin to focal adhesion complexes and since transfection of vinculin into 5.51 cells promotes stress fiber formation by stabilizing focal adhesions (cf. [14]), we believe that the lack of vinculin in 5.51 cells results in a decrease in overall cell elasticity. This observation is supported by previous findings, in which individual 5.51 cells as well as cell populations of $\sim 5 \times 10^6$ cells were exposed to external forces by the cantilever (AFM) and oscillating shear in the rheometer, respectively [5]. The results and data from this experiment show an average reduction in the elastic properties of 20% for vinculin-deficient (5.51) cells, compared with wild type (F9) cells. In a separate experiment, applying mechanical stresses across the transmembrane protein integrin using RGD coated magnetic beads, we measured the effects of loss of vinculin in 5.51 cells in a magnetometer [14]. Here, we found that the absence of vinculin correlated with a decrease in local mechanical stiffness by almost 50% compared with that of wild type cells. Thus, when vinculin was replaced by transfection in 5.51 cells, stiffness increased in 5.51_{Vin3} cells

and reached almost wild type level in 5.51_{Vin4} cells. More recently, we examined the F9Vin(−/−) cell line, in which both vinculin genes are inactivated by homologous recombination [8]. Using the magnetometer to measure local stiffness and the atomic force microscope to image the elastic distribution in whole cells, we showed that the lack of vinculin decreased the local stiffness by about 21% and the overall elasticity by almost 20% in comparison with wild type cells. These physical parameters were restored to nearly wild type level by transfecting F9Vin(−/−) cells with the vinculin gene expressing $\geq 83\%$ intact vinculin. Thus transfecting F9Vin(−/−) cells expressing vinculin devoid of the first 288 amino acids, or devoid of the active phosphorylation site (aa 822) on vinculin, resulted in only partial recovery of the phenotype and the cell's physical properties.

All in all, these experiments show (a) that the results from both vinculin-deficient cell lines, F9Vin(−/−) and 5.51, are comparable, despite the reduced expression of uvomorulin in 5.51 cells; and (b) that the applied methods provide an 'experimental handle' that can be used to define the role of vinculin in cytoskeleton-membrane coupling.

Acknowledgements: We are grateful to Dr. Eileen Adamson for providing the cells and Dr. Markus Ziegler and Ulrich Schultheiss for helpful comments. We also thank Judith Feldmann for careful reading of the manuscript. This work was supported by the American Cancer Society, Deutsche Forschungsgemeinschaft (Go 598/3-1) and NATO (CRG 970205). Excerpts of this work were presented at the annual ASCB Meeting (1997) in Washington as a poster and published in abstract form in *Mol. Biol. Cell*, 8:S, 77a.

References

- [1] Goldmann, W.H., Ezzell, R.M., Adamson, E.D., Niggli, V. and Isenberg, G. (1996) *J. Muscle Res. Cell Motil.* 17, 1–5.
- [2] Grover, A., Rosentraus, M.J., Sterman, B., Snook, M.E. and Adamson, E.D. (1987) *Dev. Biol.* 120, 1–11.
- [3] Samuels, M., Ezzell, R.M., Cardozo, T.J., Critchley, D.R., Coll, J.L. and Adamson, E.D. (1993) *J. Cell Biol.* 121, 909–921.
- [4] Goldmann, W.H., Schindl, M., Cardozo, T.J. and Ezzell, R.M. (1995) *Exp. Cell Res.* 221, 311–319.
- [5] Goldmann, W.H. and Ezzell, R.M. (1996) *Exp. Cell Res.* 226, 234–237.
- [6] Coll, J.L., Ben-Ze'ev, A., Ezzell, R.M., Rodriguez Fernandez, J.L., Baribault, H., Oshima, R.G. and Adamson, E.D. (1995) *Proc. Natl. Acad. Sci. USA* 92, 9161–9165.
- [7] Volberg, T., Geiger, B., Kam, Z., Pankov, R., Simcha, I., Sabanay, H., Coll, L.J., Adamson, E.D. and Ben-Ze'ev, A. (1995) *J. Cell Sci.* 108, 2253–2260.
- [8] Goldmann, W.H., Galneder, R., Ludwig, M., Xu, W., Adamson, E.D., Wang, N. and Ezzell, R.M. (1998) *Exp. Cell Res.* 239 (in press).
- [9] Schindl, M., Wallraff, E., Deubzer, B., Witke, W., Gerisch, G. and Sackmann, E. (1995) *Biophys. J.* 68, 1177–1190.
- [10] Ziegler, M. (1995) PhD Thesis, Technical University of Munich.
- [11] Duszyk, M., Schwab III, B., Zahalak, G.I., Qian, H. and Elson, E.L. (1989) *Biophys. J.* 55, 683–690.
- [12] Schultheiss, U. (1996) MSc Thesis, Technical University of Munich.
- [13] Radmacher, M., Fritz, M., Kacher, C.M., Cleveland, J.P. and Hansma, P.K. (1996) *Biophys. J.* 70, 556–567.
- [14] Ezzell, R.M., Goldmann, W.H., Wang, N., Parasharama, N. and Ingber, D.E. (1997) *Exp. Cell Res.* 231, 14–26.
- [15] Wang, N., Butler, J.P. and Ingber, D.E. (1993) *Science* 260, 1124–1127.